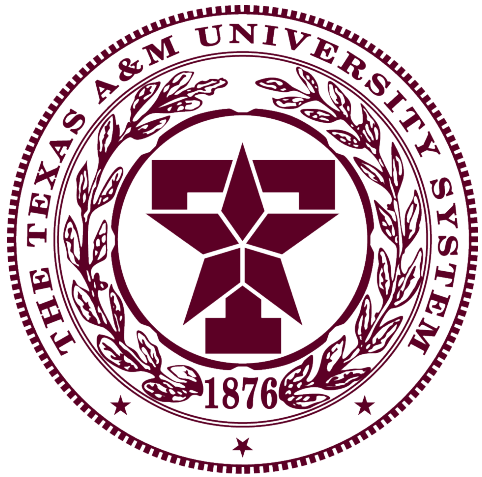

Neutron Flux Characterization in TRIGA Large Irradiation Cell

James B. Tompkins & Ryan G. McClarren

Test, Research, and Training Reactors (TRTR) 2016
Albuquerque, NM

Texas A&M University

NSC Large Irradiation Cell

- Unique experiment position at Texas A&M Nuclear Science Center
- 16 ft by 18 ft open area accomodating samples of various size
- Irradiation cell experiment source options:
  - 1 MW TRIGA reactor (neutron/gamma dose in spectrum)
  - Rechargable lanthanum source (limited energy gamma dose)
- High spatial dependence for neutron flux
  - Allows experiment flexibility
  - Lack of flux model for cell leads to large uncertainty in sample dose
- Need to characterize neutron flux in cell

PDT

- Texas A&M's massively parallel deterministic transport code
  - Scales on logically Cartesian grids out to 750,000 cores
- Angular discretization using discrete ordinates
- Simulation Capabilities:
  - Multi-group
  - Steady-state and time-dependent
  - Criticality and depletion problems
- Radiation Models:
  - Neutron
  - Gamma
  - Electron
  - Coupled neutron-gamma
  - Coupled electron-photon

Motivations

- 1. NSC's need for computational model
  - Experimenters expect consistent results and/or have sensitive samples.
  - Model of cell would increase confidence in experiment results.
- 2. PDT's need for validation cases
  - PDT is rapidly maturing as a transport code.
  - To grow user base, need to demonstrate results reflect reality.
- Large irradiation cell model benefits both programs.

Model Development and Validation Methods

- Model Development
  - Cell Geometry
    - Measure cell
    - Develop Cartesian mesh
  - Material properties
    - Densities
    - Microscopic cross sections
  - Develop boundary condition
    - Fit surface from data collected
    - Discretize in angle
- Model Validation
  - Perturb boundary condition using surface fit statistics
  - Compare computational results to experiment data

The Steady-State Transport Equation

$$\vec{\Omega}\cdot\vec{\nabla}\psi(\vec{r},E,\vec{\Omega})+\Sigma_t(\vec{r},E)\psi(\vec{r},E,\vec{\Omega})=$$
$$\int_0^\infty dE'\int_{4\pi}d\Omega'\Sigma_s(\vec{r},E'\rightarrow E,\Omega'\rightarrow\Omega)\psi(\vec{r},E',\vec{\Omega}')+S_{ext}(\vec{r},E,\vec{\Omega})$$

$$\vec{\Omega}\cdot\vec{\nabla}\psi(\vec{r},E,\vec{\Omega})+\Sigma_t(\vec{r},E)\psi(\vec{r},E,\vec{\Omega})=$$
$$\frac{1}{4\pi}\int_0^\infty dE'\Sigma_s(\vec{r},E'\rightarrow E)\int_{4\pi}d\Omega'\psi(\vec{r},E',\vec{\Omega}')+S_{ext}(\vec{r},E,\vec{\Omega})$$
$$=\frac{1}{4\pi}\int_0^\infty dE'\Sigma_s(\vec{r},E'\rightarrow E)\phi(\vec{r},E')+S_{ext}(\vec{r},E,\vec{\Omega})$$

The Multigroup Transport Equation

$$\phi(\vec{r}, E') = \int_{4\pi} d\Omega' \psi(\vec{r}, E', \vec{\Omega}')$$

$$\vec{\Omega} \cdot \vec{\nabla} \psi_g(\vec{r}, \vec{\Omega}) + \Sigma_{t,g}(\vec{r}) \psi_g(\vec{r}, \vec{\Omega}) = \frac{1}{4\pi} \sum_{g'} \Sigma_{s,g' \to g}(\vec{r}) \phi_{g'}(\vec{r}) + S_{ext,g}(\vec{r}, \vec{\Omega}),$$

$$\text{for } 1 \leq g \leq G$$

The Discrete Ordinates Transport Equation

$$\vec{\Omega}_m \cdot \vec{\nabla}\psi_{g,m}(\vec{r}) + \Sigma_{t,g}(\vec{r})\psi_{g,m}(\vec{r}) = \frac{1}{4\pi}\sum_{g'}\Sigma_{s,g'\rightarrow g}(\vec{r})\phi_{g'}(\vec{r}) + S_{ext,g,m}(\vec{r})$$

$$\phi_g(\vec{r}) \approx \sum_{m=1}^{m=M} w_m \psi_{g,m}(\vec{r}).$$

Input to Construct Model

With the transport equation discretized, three inputs are necessary to model a problem:

- problem geometry: a mesh upon which to solve the problem
- material properties: density and group averaged cross sections
- boundary condition: the angular flux incident upon boundaries
  - By position (x, y, z)
  - By solid angle (μ, η, ξ)

Cell Geometry

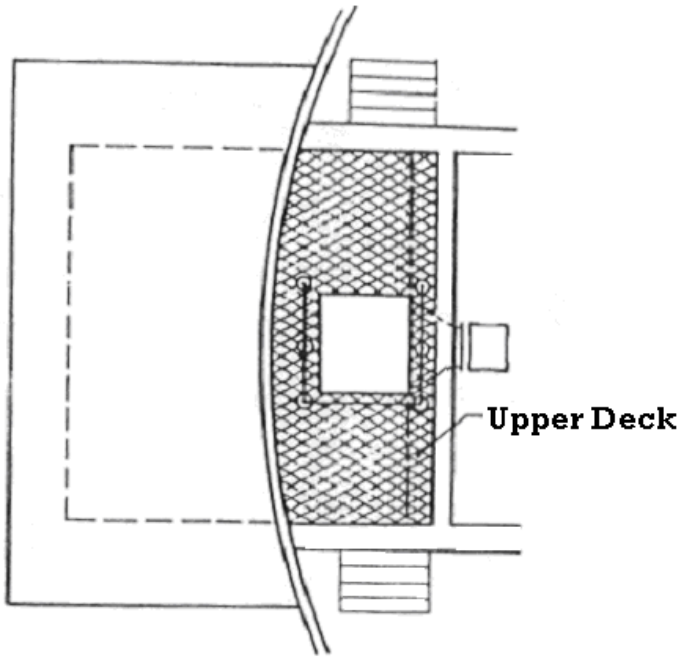

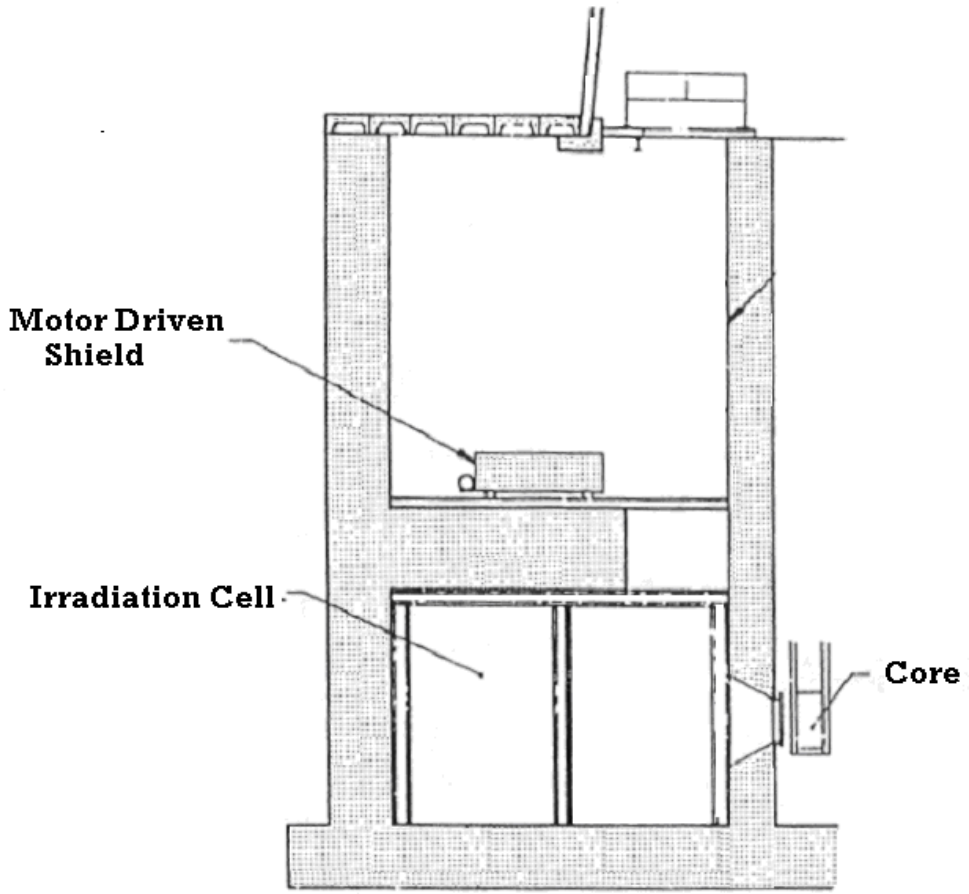

Cell Geometry Discretization

- Physically measure the cell's space
- Develop Cartesian mesh
  - Irradiation cell divided into largest blocks of same material
  - Blocks become material regions
  - Some approximations necessary (e.g. slanted walls around window)
  - Material regions divided into cells based upon:
    - desired spatial resolution (largest cell volumes)
    - ability for dimensions to be evenly divided to run in parallel.

Material Properties

- Macroscopic group-averaged cross section comes from
  - Density
  - Microscopic group-averaged cross section
- Material specifications detail
  - Density
  - Chemical Composition
- Cross section processing
  - Unprocessed microscopic cross sections obtained from OECD JANIS
  - ENDF/B-VII.0 libraries
  - Find cross sections for isotopes in each element in cell materials
  - Collapsed into groups based on experiment activation material
  - Group processing uses TRIGA experimental flux spectrum

PDT Model Specifications

- Computational Methods
  - Geometry solve: Piecewise linear discontinuous (PWLD) method
  - Unlumped PWLD version
  - Group set iteration: generalized minimal residual method (GMRES)
  - Angle set iteration: Richardson
- Intermediate neutron boundary source
  - Angles overlooked in reactor point approximation analysis
  - Neutrons incident upon the cell from positions not able to be measured
  - Can be considered an experiment calibration parameter

Neutron Activation Experiments

- Flux foil advantages
  - Size small enough to give pointwise flux evaluations
  - Through foil stacks, can bound energy groups
- Foil configuration
  - Gold-aluminum (0.027% Au) bare and cadmium covered stacked foils
  - Primary neutron activation material: gold
  - Cadmium shields covered foil from thermal neutron dose
- Detection method
  - Need a detector capable of energy resolution
  - NSC counting lab has high purity germanium (HPGe) detectors
  - HPGe: inorganic scintillator with high energy resolution

$$\phi = \frac{A(t)\lambda}{\sigma N_o} \frac{e^{\lambda t_{decay}}}{(1 - e^{-\lambda t_{irr}})}$$

Flux Collection Experiments

- Two types of flux data collected:
  - Model Development Data (on cell window)
  - Model Validation Data (throughout cell)
- Experiment Procedure
  - Foil stacks placed in cell, and cell is sealed with movable shield
  - Void box installed on reactor west face
  - Reactor positioned outside irradiation cell window
  - TRIGA run at 1 MW for 45 minutes
  - Operate only after at least two day down period (Monday mornings)
  - Limiting operation minimizes short lived fission products (e.g. ^{135}Xe)

Boundary Condition Development Experiment Data

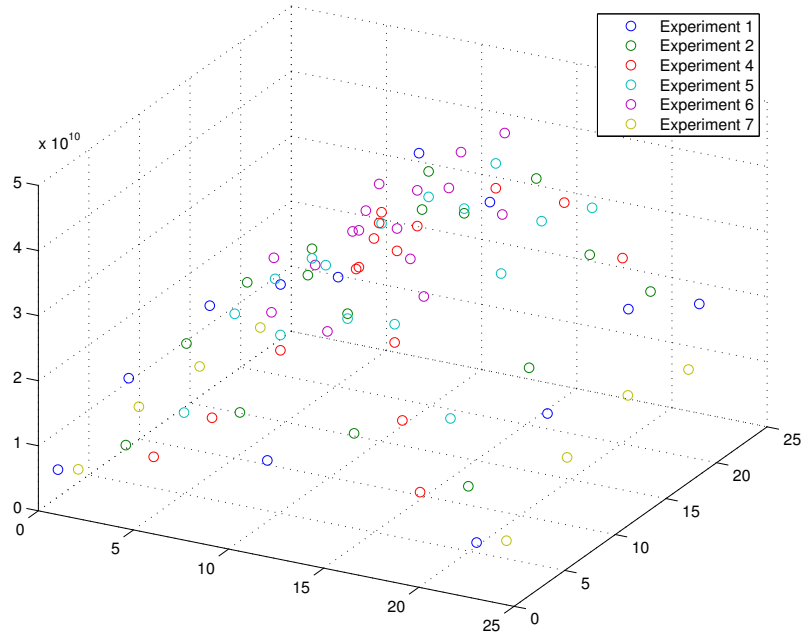

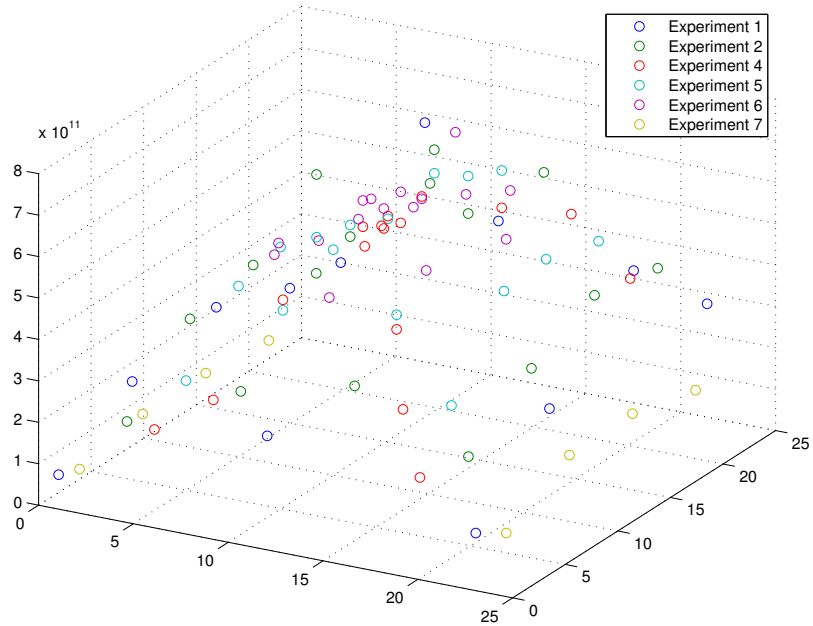

Validation Experiment Data Collection Points

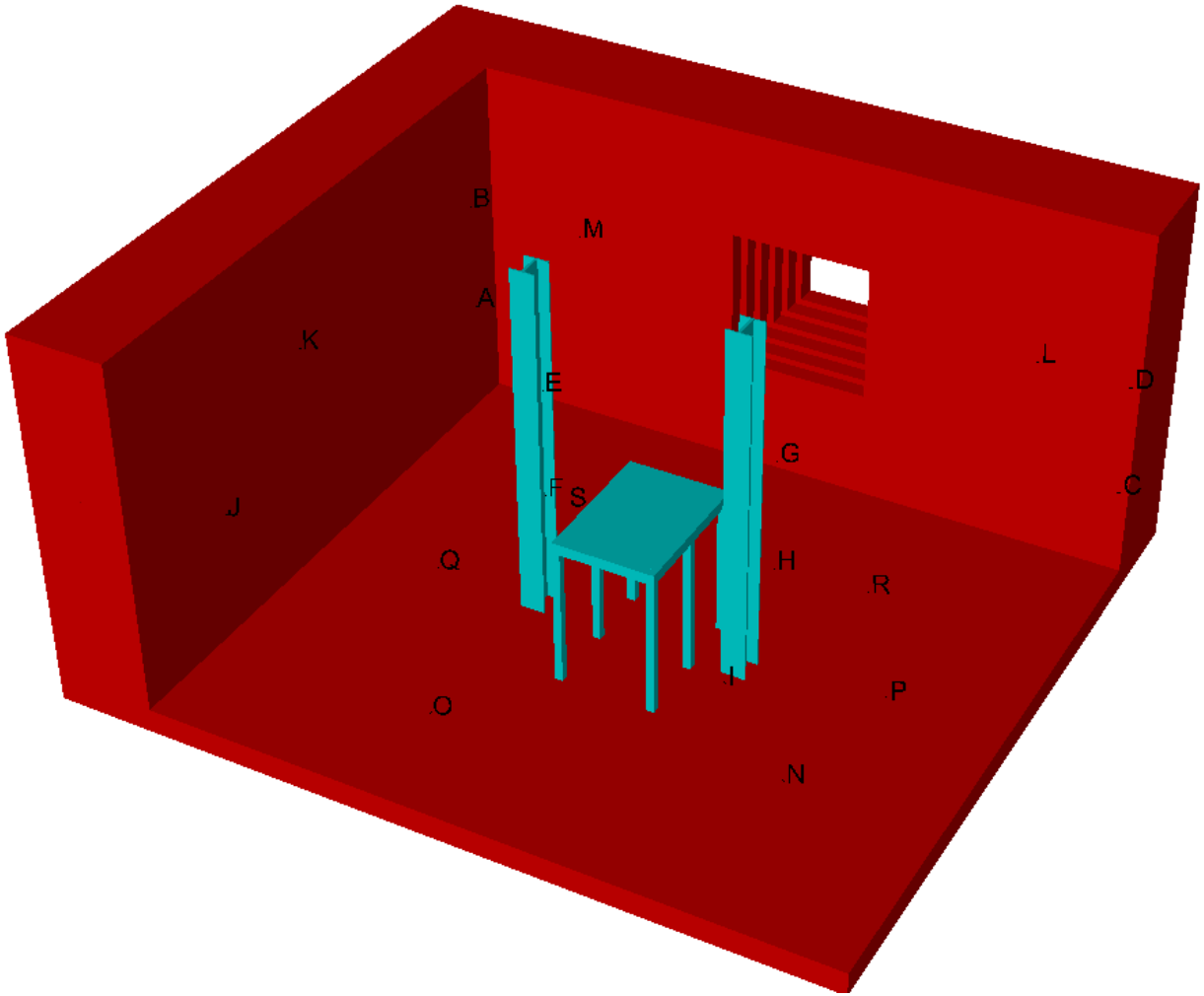

Flux Fitting on Window Surface

- Now have flux magnitudes at various points on the window surface
- Need flux at vertices on cell boundary to specify incident flux
- Flux at vertices needs to be provided regardless of geometric resolution
- Flux data fit to surfaces
  - Two surfaces generated (one for each energy group)
  - Fitting method is locally weighted regression (lowess)
  - Regression methods fit data to nominal surface
  - Statistical nature of regression fitting
    - Confidence interval to bound experiment data
    - Standard Error of generated data points

Flux Fitting Results

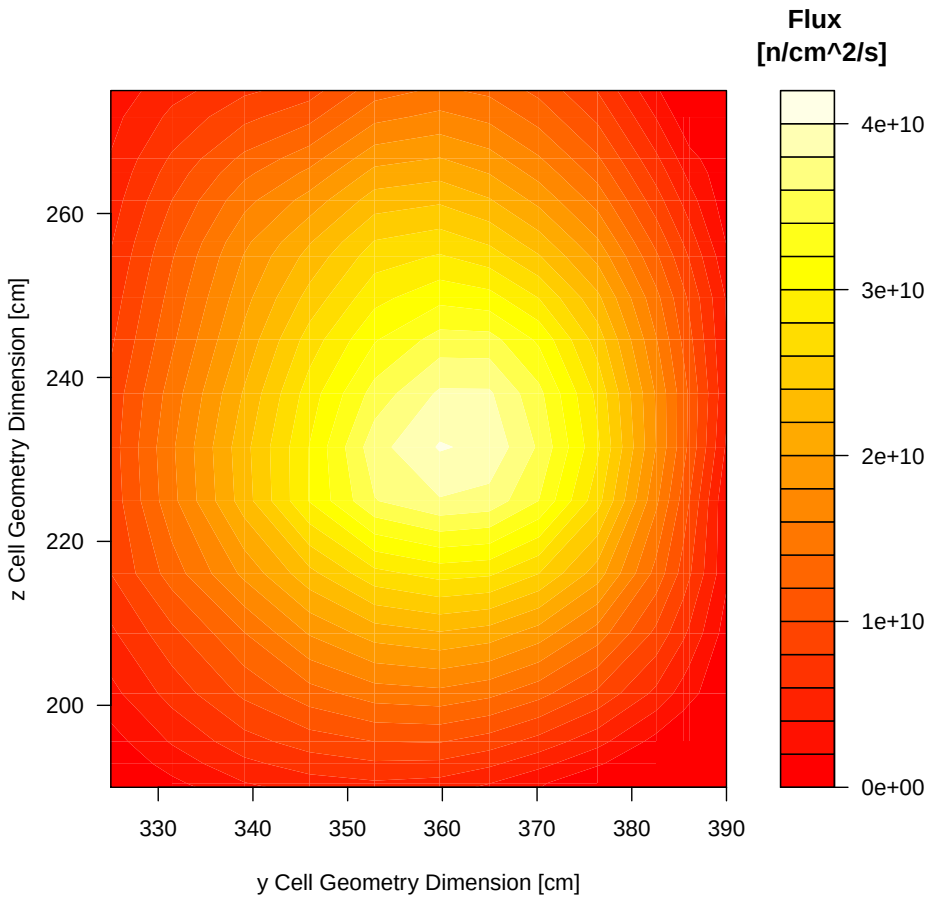

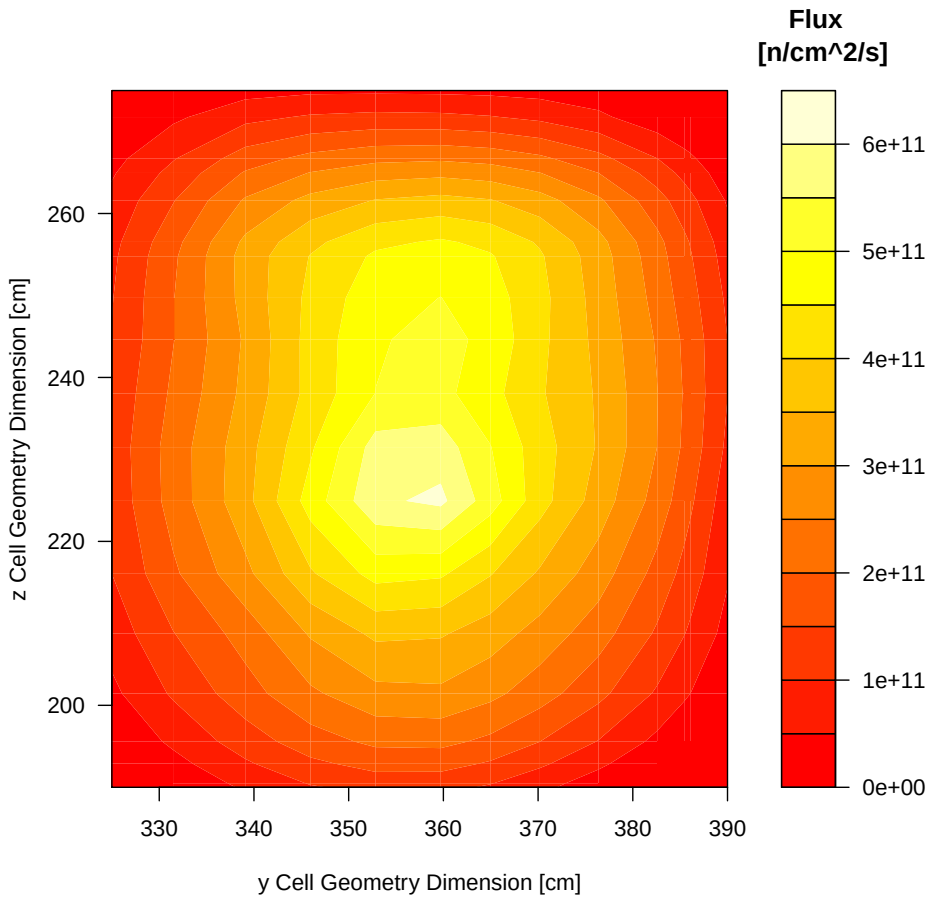

Angular Discretization

- Solution method requires specification of BC angular distribution
- Data suggests flux on cell boundary is not isotropic
- Incident flux must be distributed in angle
  - Identify location of source in relation to geometry of cell boundary
  - Point source approximation of TRIGA emissions (MCNP modeled)
  - Calculate attenuated flux from each point source via ray tracing
  - Compare calculated flux with validation data at experiment points
  - Vary reactor model position to find optimal reactor location
  - Use reactor location to calculate solid angles through vertices
  - Weights for each angle at each point are ratio of flux passing through a solid angle to total flux passing through point
  - Calculated angles probably not in quadrature set (angular disc. for S_n)
  - Calculated angles matched to closest quadrature angle
  - Matched angles' weights added to that angle in quadrature
  - Quadrature used: medium level LDFE (2048 angles)

Nominal Epithermal Cell Flux Visualization

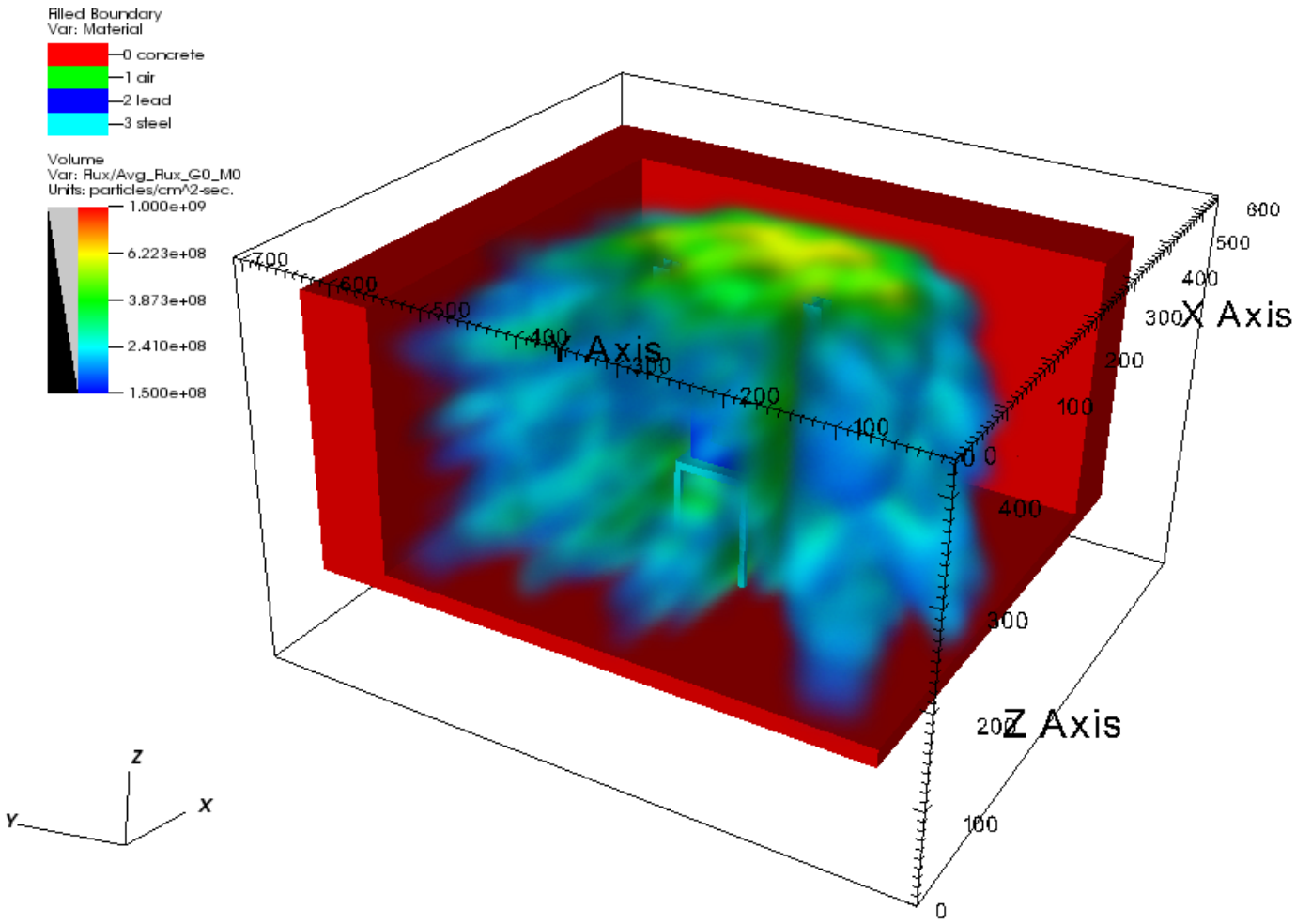

Nominal Thermal Cell Flux Visualization

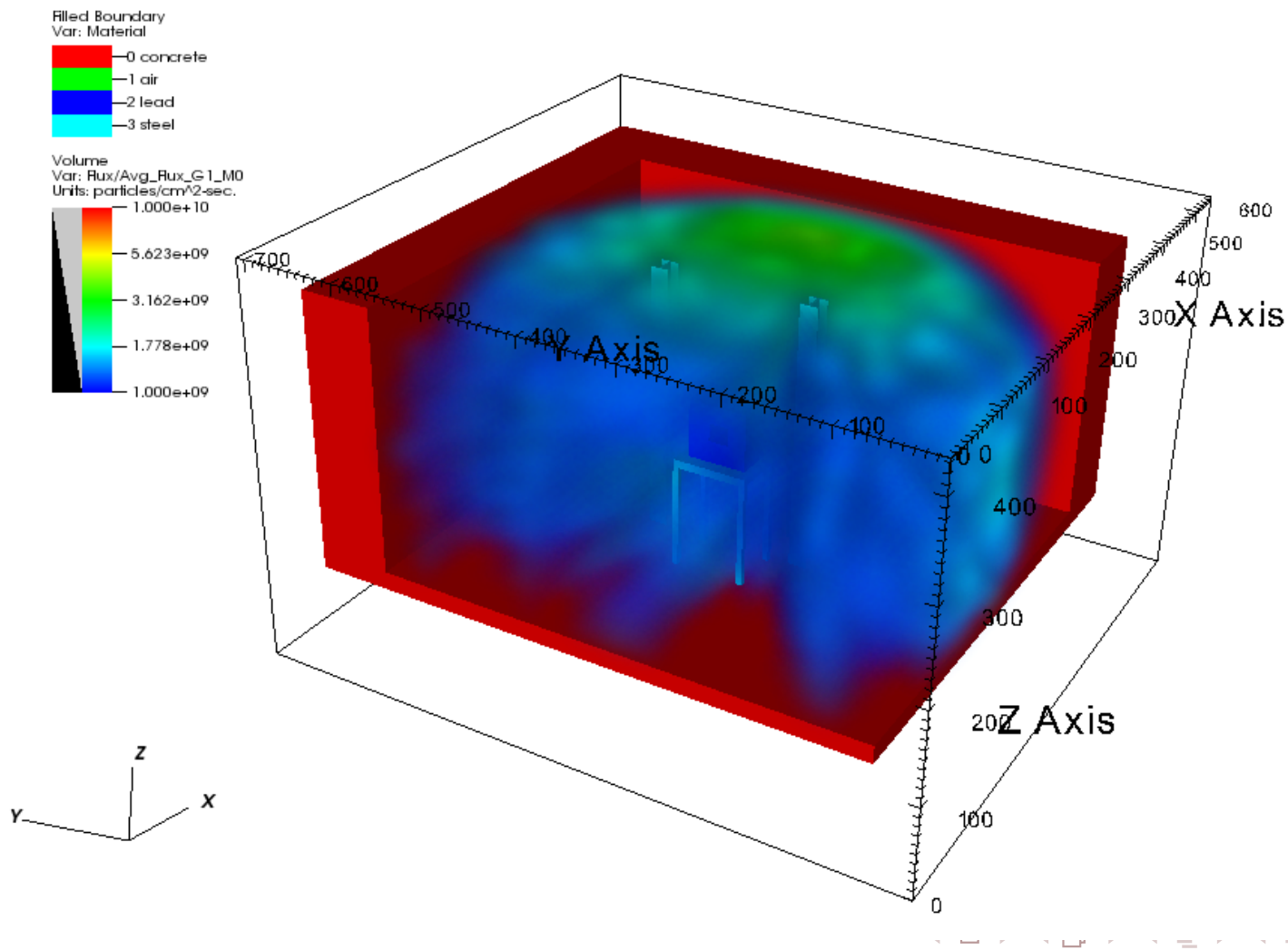

Nominal Epithermal Result Comparison Plot

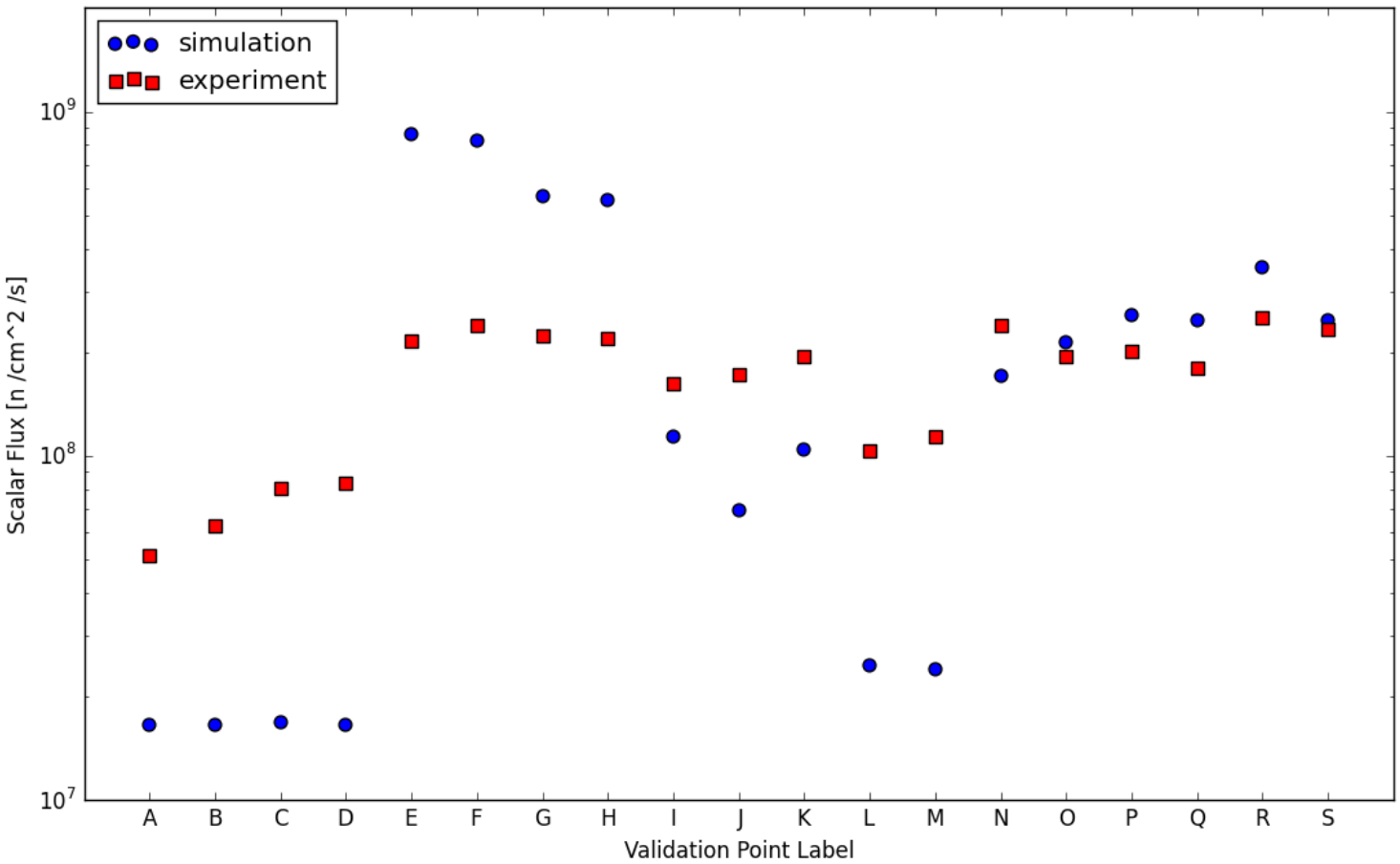

Nominal Thermal Result Comparison Plot

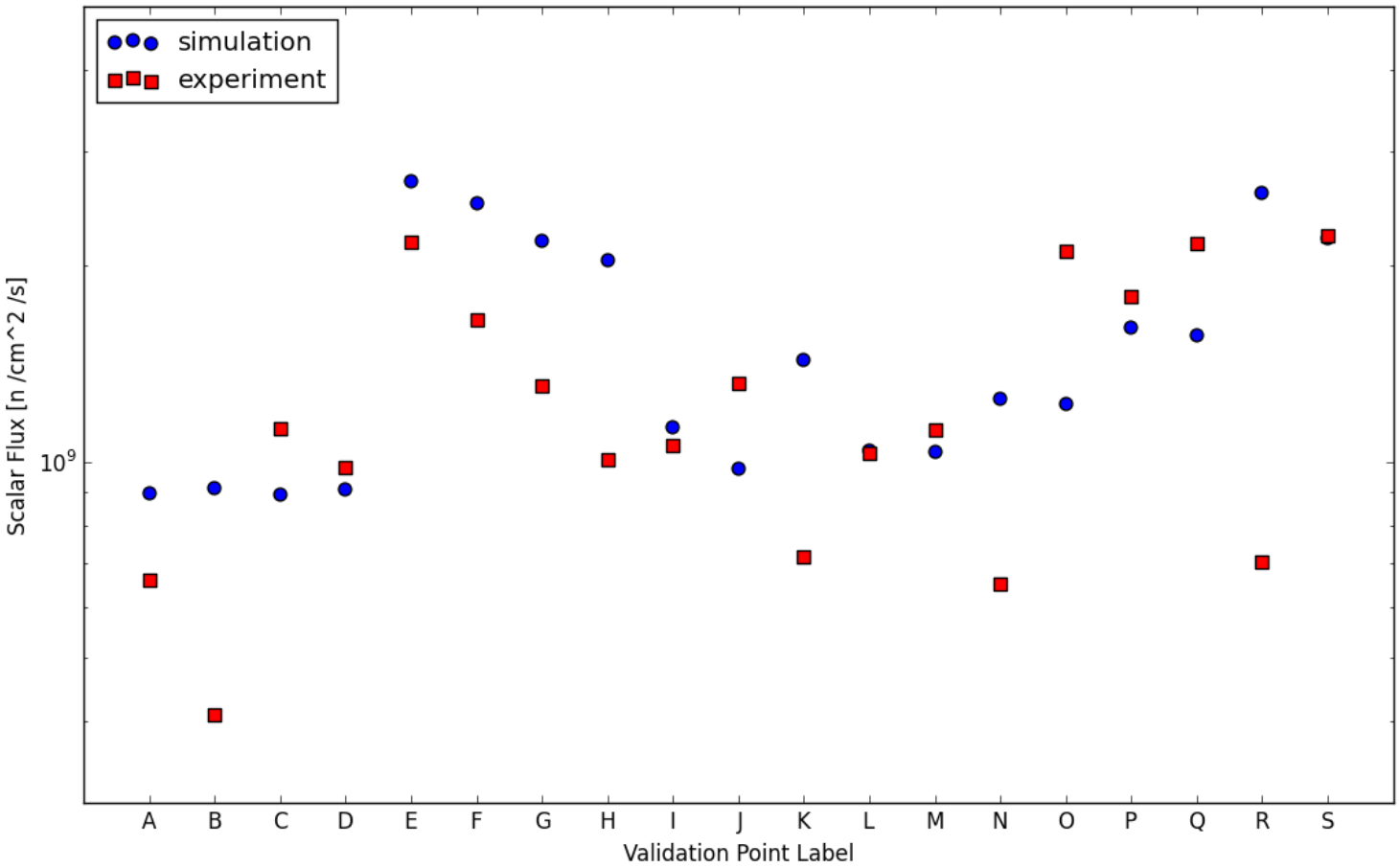

Validation Method

- Experiment data is compared to simulation results
- Need to determine simulated results plausibility
- Perturb boundary condition to establish computational bounds
- Can use normal distribution with
  - Mean: nominal fitted values of surface fits
  - Standard Dev.: standard error of fitted magnitudes
- Sample distribution and run simulations to develop computational bounds
- Goal of bounding experiment validation data within perturbed results

Input Perturbation and Result Collection

- Heron PDT UQ Framework
  - Samples distributions
  - Generates perturbed input files
  - Schedules jobs to run on various systems
  - Collects results for analysis
- Sampling accomplished with Numpy's random package
- Sampled variables are injected into input file template using tags (similar to DAKOTA)
- Parses PDT output files for cell averaged flux at given position

Epithermal Validation Results Plot

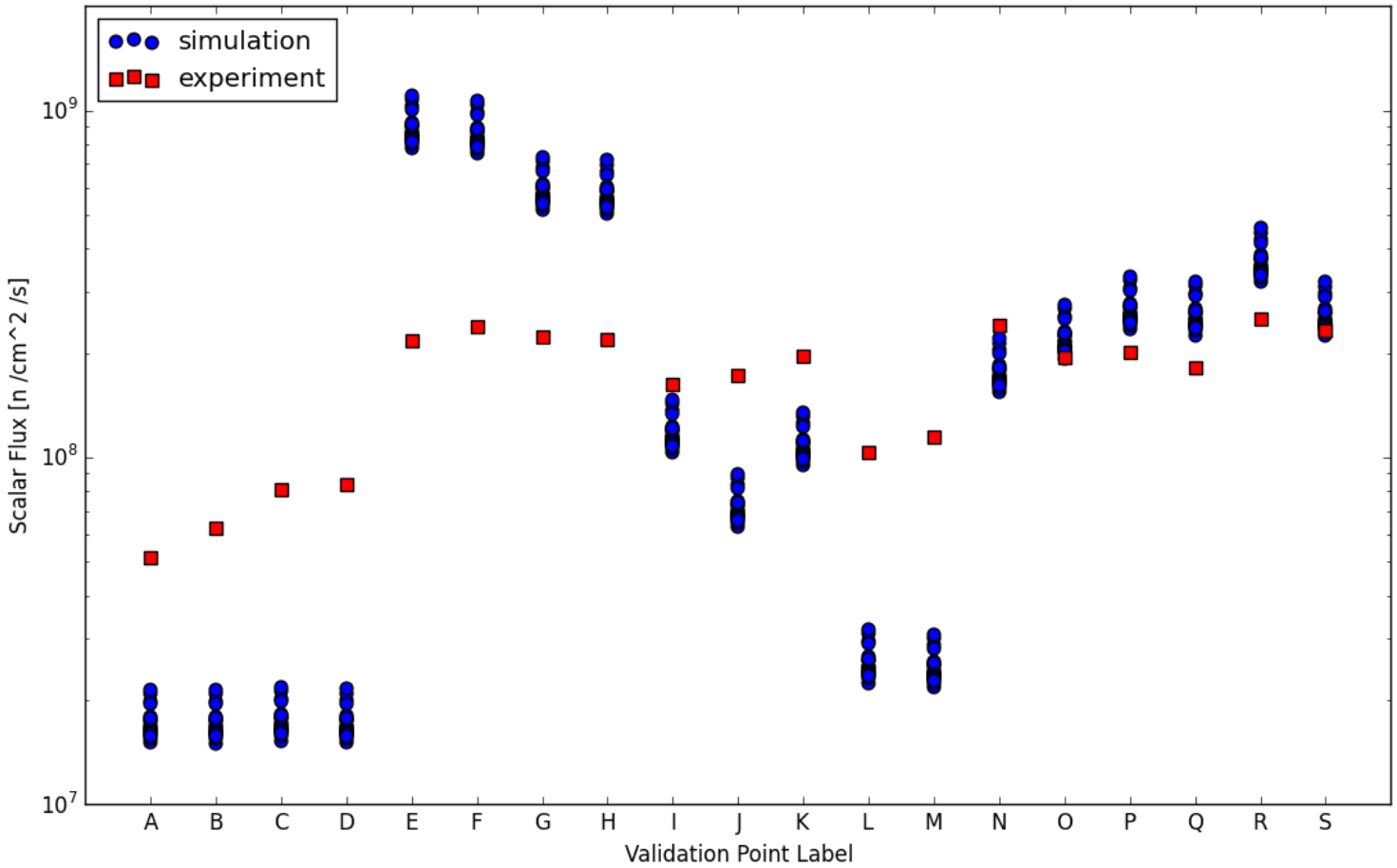

Thermal Validation Results Plot

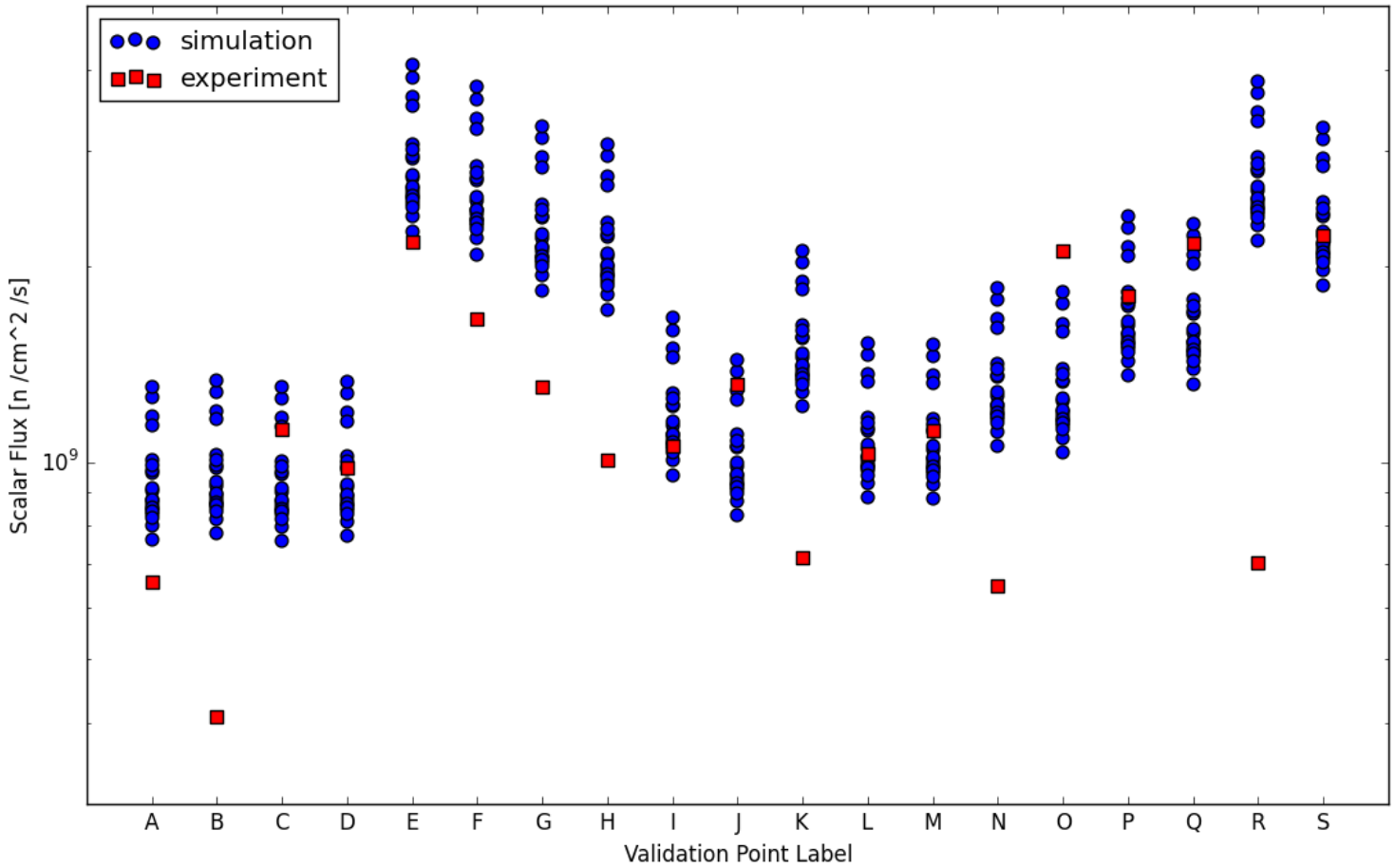

Development Model Comparisons

- To determine which aspects of the model are driving the fully developed model, simulations with simpler formulations are run.
- Two models compared to experiment data and fully developed model
  - Isotropic boundary source neglecting spatial distribution (one flux magnitude value across boundary)
  - Isotropic angular distribution on boundary with spatially flux distribution

Epithermal Model Comparison Plot

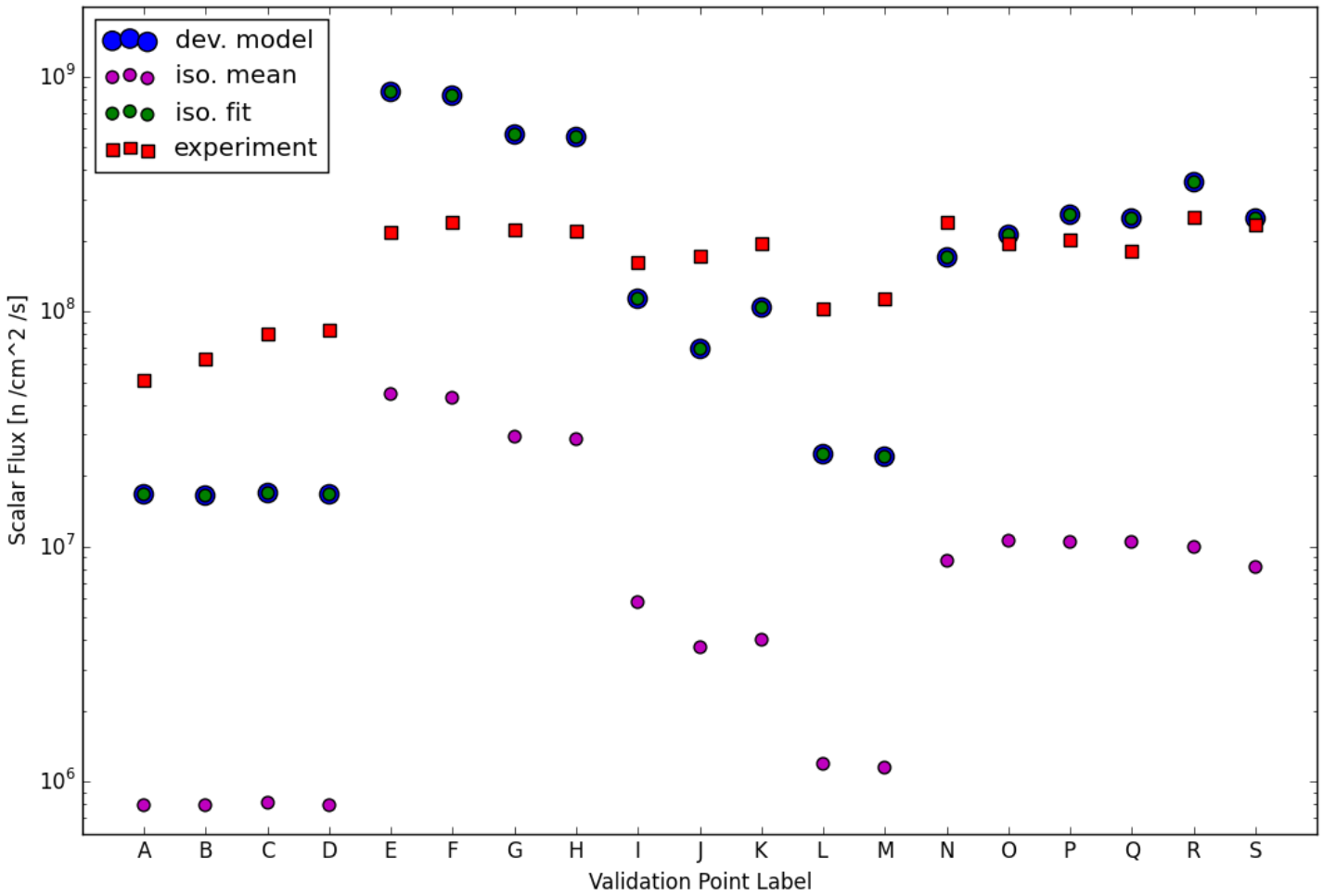

Thermal Model Comparison Plot

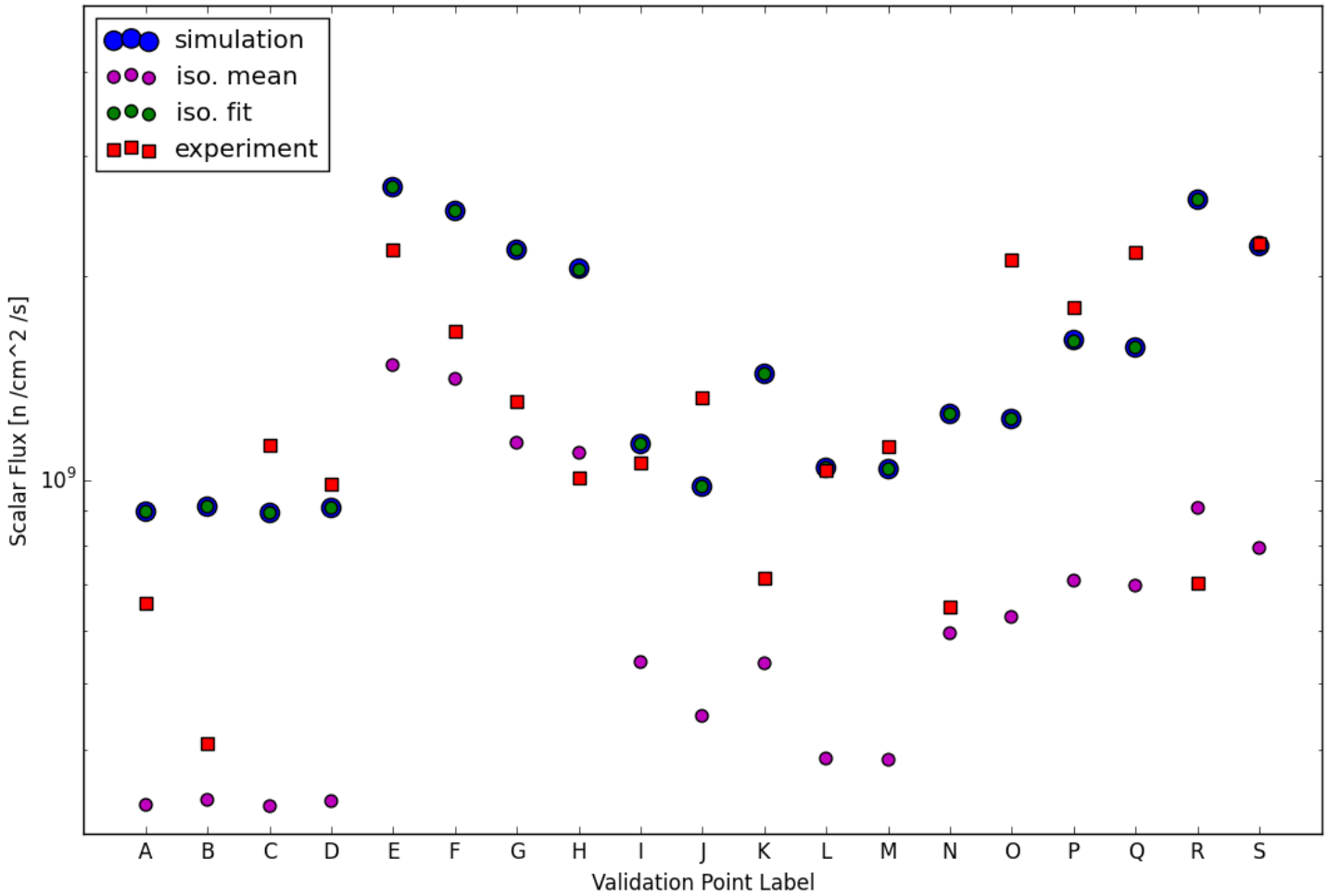

Conclusions

- Epithermal results appear to be overestimated within view and closer to the window (points E-H) and underestimated at points towards the edges of the cell out of view of the window (A-D,I,J). Further away from the window, the model predicts flux more accurately and several points fall within the computational validation bounds (N,O,S).
- Thermal results are more promising. Points close to and within view of the window are still overestimated in this energy region (E-H), but edge points are either overestimated (A,B) or fall within the validation bounds (C,D,I,J). Over half of the calculated thermal flux experiment points fall within the validation bounds inspiring confidence for futher work.

Future Work

- Extend data collection scope to include flux for higher energies.
- Propagate measurement errors through to cell model.
- Vary reactor position via
  - perturbation of BC flux magnitude and angular distribution.
  - adjusting extents of the intermediate neutron boundary source.
- Collect more validation points.
- Increased scattering level (only P0 scattering cross sections currently).

Nominal Epithermal Result Comparison Table

Position No.	Foil Cell Position [cm]			Epithermal Scalar Flux [n cm^{-2} s^{-1}]	
	x	y	z	Experimental	Computational
A	452.12	548.64	91.44	5.1242e+07	1.6580e+07
B	452.12	548.64	182.88	6.2608e+07	1.6557e+07
C	452.12	0	91.44	8.0885e+07	1.6851e+07
D	452.12	0	182.88	8.3702e+07	1.6633e+07
E	251.46	365.91875	182.88	2.1637e+08	8.5683e+08
F	251.46	365.91875	91.44	2.3925e+08	8.2701e+08
G	251.46	180.49875	182.88	2.2259e+08	5.6947e+08
H	251.46	180.49875	91.44	2.1900e+08	5.5567e+08
I	0	91.44	203.2	1.6239e+08	1.1383e+08
J	0	457.2	203.2	1.7307e+08	6.9482e+07
K	215.9	548.64	182.88	1.9514e+08	1.0459e+08
L	482.6	81.28	162.56	1.0328e+08	2.4694e+07
M	482.6	467.36	162.56	1.1410e+08	2.3960e+07
N	147.32	119.38	0	2.3979e+08	1.7014e+08
O	93.98	370.84	0	1.9470e+08	2.1311e+08
P	261.62	93.98	0	2.0152e+08	2.5751e+08
Q	241.3	457.2	0	1.8068e+08	2.4820e+08
R	368.3	157.48	0	2.5158e+08	3.5402e+08
S	358.14	411.48	0	2.3297e+08	2.4758e+08

Nominal Thermal Result Comparison Table

Position No.	Foil Cell Position [cm]			Thermal Scalar Flux [n cm^{-2} s^{-1}]	
	x	y	z	Experimental	Computational
A	452.12	548.64	91.44	6.5816e+08	8.9599e+08
B	452.12	548.64	182.88	4.0887e+08	9.1307e+08
C	452.12	0	91.44	1.1263e+09	8.9241e+08
D	452.12	0	182.88	9.8333e+08	9.0853e+08
E	251.46	365.91875	182.88	2.1798e+09	2.6961e+09
F	251.46	365.91875	91.44	1.6573e+09	2.4924e+09
G	251.46	180.49875	182.88	1.3071e+09	2.1849e+09
H	251.46	180.49875	91.44	1.0072e+09	2.0448e+09
I	0	91.44	203.2	1.0598e+09	1.1290e+09
J	0	457.2	203.2	1.3203e+09	9.7723e+08
K	215.9	548.64	182.88	7.1715e+08	1.4357e+09
L	482.6	81.28	162.56	1.0337e+09	1.0409e+09
M	482.6	467.36	162.56	1.1199e+09	1.0360e+09
N	147.32	119.38	0	6.4910e+08	1.2527e+09
O	93.98	370.84	0	2.1073e+09	1.2270e+09
P	261.62	93.98	0	1.7991e+09	1.6083e+09
Q	241.3	457.2	0	2.1662e+09	1.5637e+09
R	368.3	157.48	0	7.0266e+08	2.5872e+09
S	358.14	411.48	0	2.2265e+09	2.2081e+09

Epithermal Validation Results Table

Position No.	Foil Cell Position [cm]			Epithermal Scalar Flux [n cm^{-2} s^{-1}]		
	x	y	z	Experimental	Min Computational	Max Computational
A	452.12	548.64	91.44	5.1242e+07	1.5027e+07	2.1431e+07
B	452.12	548.64	182.88	6.2608e+07	1.5007e+07	2.1402e+07
C	452.12	0	91.44	8.0885e+07	1.5273e+07	2.1780e+07
D	452.12	0	182.88	8.3702e+07	1.5075e+07	2.1499e+07
E	251.46	365.91875	182.88	2.1637e+08	7.7657e+08	1.1075e+09
F	251.46	365.91875	91.44	2.3925e+08	7.4954e+08	1.0690e+09
G	251.46	180.49875	182.88	2.2259e+08	5.1615e+08	7.3600e+08
H	251.46	180.49875	91.44	2.1900e+08	5.0363e+08	7.1825e+08
I	0	91.44	203.2	1.6239e+08	1.0317e+08	1.4713e+08
J	0	457.2	203.2	1.7307e+08	6.2973e+07	8.9812e+07
K	215.9	548.64	182.88	1.9514e+08	9.4789e+07	1.3519e+08
L	482.6	81.28	162.56	1.0328e+08	2.2381e+07	3.1918e+07
M	482.6	467.36	162.56	1.1410e+08	2.1716e+07	3.0970e+07
N	147.32	119.38	0	2.3979e+08	1.5422e+08	2.1986e+08
O	93.98	370.84	0	1.9470e+08	1.9315e+08	2.7546e+08
P	261.62	93.98	0	2.0152e+08	2.3342e+08	3.3275e+08
Q	241.3	457.2	0	1.8068e+08	2.2495e+08	3.2082e+08
R	368.3	157.48	0	2.5158e+08	3.2086e+08	4.5760e+08
S	358.14	411.48	0	2.3297e+08	2.2439e+08	3.2002e+08

Thermal Validation Results Table

Position No.	Foil Cell Position [cm]			Thermal Scalar Flux [n cm^{-2} s^{-1}]		
	x	y	z	Experimental	Min Computational	Max Computational
A	452.12	548.64	91.44	6.5816e+08	7.6376e+08	1.3090e+09
B	452.12	548.64	182.88	4.0887e+08	7.7834e+08	1.3339e+09
C	452.12	0	91.44	1.1263e+09	7.6074e+08	1.3037e+09
D	452.12	0	182.88	9.8333e+08	7.7451e+08	1.3272e+09
E	251.46	365.91875	182.88	2.1798e+09	2.2578e+09	4.0653e+09
F	251.46	365.91875	91.44	1.6573e+09	2.0860e+09	3.7618e+09
G	251.46	180.49875	182.88	1.3071e+09	1.8349e+09	3.2784e+09
H	251.46	180.49875	91.44	1.0072e+09	1.7158e+09	3.0726e+09
I	0	91.44	203.2	1.0598e+09	9.5756e+08	1.6645e+09
J	0	457.2	203.2	1.3203e+09	8.3046e+08	1.4357e+09
K	215.9	548.64	182.88	7.1715e+08	1.2193e+09	2.1116e+09
L	482.6	81.28	162.56	1.0337e+09	8.8706e+08	1.5214e+09
M	482.6	467.36	162.56	1.1199e+09	8.8286e+08	1.5143e+09
N	147.32	119.38	0	6.4910e+08	1.0605e+09	1.8532e+09
O	93.98	370.84	0	2.1073e+09	1.0356e+09	1.8247e+09
P	261.62	93.98	0	1.7991e+09	1.3595e+09	2.3857e+09
Q	241.3	457.2	0	2.1662e+09	1.3207e+09	2.3227e+09
R	368.3	157.48	0	7.0266e+08	2.1875e+09	3.8355e+09
S	358.14	411.48	0	2.2265e+09	1.8702e+09	3.2638e+09